Cation Identity Affects Nonadditivity in Salt Mixtures Containing Iodide and Sulfate

Pho T. Bui[1] and Paul S. Cremer[1,2]*

[1]*Department of Chemistry and* [2]*Department of Biochemistry and Molecular Biology, The Pennsylvania State University, University Park, PA 16802, USA.*

*Corresponding author: P.S.C. psc11@psu.edu

P.T.B. https://orcid.org/0000-0003-2722-5982
P.S.C. https://orcid.org/0000-0002-8524-0438

Abstract

The cloud point temperature of poly(*N*-isopropylacrylamide) (PNIPAM) was measured in aqueous solutions containing salt mixtures. Solutions were made with SO_4^{2-}, a strongly hydrated anion, I^-, a weakly hydrated anion, or both anions together with a common alkali metal counterion: Li^+, Na^+, K^+ or Cs^+. Nonadditive behavior was observed when the MI concentration was increased in the presence of 0.2 mol·L^{-1} M_2SO_4. Although complex changes in the cloud point temperature were observed with all four metal counter cations, the magnitude of the effects differed substantially amongst them. More specifically, SO_4^{2-} was able to swipe cations away from I^- in each case, but its propensity to do so depended on the relative strength of the cation-iodide versus the cation-sulfate interactions. When the counterion was stripped away from it, I^- became more hydrated and acted more like a strongly hydrated anion. A competitive binding model was employed to determine the fraction of cations bound to SO_4^{2-} in the presence of I^-, allowing for a qualitative comparison of the fraction of strongly hydrated I^- ions that was produced with all four cations. K^+ showed the greatest relative affinity for SO_4^{2-}. As such, experiments performed with this cation led to the greatest fraction of I^- that was more hydrated and displayed the strongest nonadditive behavior. By contrast, Cs^+ showed the weakest relative affinity for SO_4^{2-}, resulting in the least pronounced nonadditivity. This work demonstrates that the identity of the counter cation plays a critical role in the nonadditive behavior of salt mixtures when both weakly and strongly hydrated anions are present.

Keywords: nonadditivity, ion-pairing, competitive binding, cations, anions, thermoresponsive polymer

Declarations

Funding: This work was funded by the National Science Foundation (CHE-2004050).
Conflict of interest: The authors declare no competing financial interest.
Availability of data and materials: Data presented in this manuscript could be provided upon request.
Code availability: Not applicable.

1 Introduction

The Hofmeister series ranks anions and cations according to their ability to precipitate proteins out of solutions [1–3]. The salting-out ability of anions follows the series:

$$CO_3^{2-} > SO_4^{2-} > S_2O_3^{2-} > H_2PO_4^- > F^- > Cl^- > Br^- > NO_3^- > I^- > ClO_4^- > SCN^-$$

Much effort has focused on elucidating the molecular level mechanisms underlying the anion series using both experimental and computational techniques [4–8]. It is well established that weakly hydrated anions on the right side of this series partition more favorably to nonpolar surfaces such as the air/water [9, 10] or hydrophobic polymer/water interfaces [4, 11, 12]. This accumulation leads to salting-in behavior. By contrast, strongly hydrated anions on the left side of the series are excluded from the polymer surface, driving precipitation. While the anion series has been extensively studied, mechanisms corresponding to the cation series have only begun to come into focus more recently [8, 13–15]. The typical consensus ranking of the cations for salting out polymers or proteins from water is [16]:

$$N(CH_3)_4^+ > NH_4^+ > Cs^+ > Rb^+ > K^+ > Na^+ > Li^+ > Ca^{2+} > Mg^{2+}$$

This series is typically dominated by the interactions of cations with negatively charged residues on proteins and polypeptides and is not necessarily generic [17–19]. In fact, studies performed on uncharged polymers containing peptide bonds have shown that strongly hydrated cations interact weakly but favorably with the amide oxygen, while weakly hydrated cations are more excluded from the amide moiety [8, 13–15]. Additionally, it should be noted that ion-specific effects arise not only from the extent of hydration of the ions and their relative accumulation around the macromolecule, but also from specific ion-macromolecule interactions. As such, the rank order of ions can depend on the functional groups on the macromolecule of interest as well as its molecular weights [11, 20], surface charges [21], surface roughness [22, 23] and surface curvature [24].

The additivity assumption, pioneered by Guggenheim, states that salt effects are equal to the sum of the individual contributions from the cations and the anions [25–29]. Very recently, however, examples of nonadditivity for single salts have been reported [15, 30, 31]. For salt series containing a common cation, the ability of this ion to interact with the polymer depends strongly upon the identity of the anion with which it is paired. This is because cation-anion pairing both in the bulk aqueous solution and at the polymer/water interface significantly influences cation-polymer interactions. As an example, counter anion identity dictates the extent to which guanidium cations interact with polymer surfaces [30]. In another case,

when paired with Cl^-, strongly hydrated cations (e.g., Li^+ and Ca^{2+}) accumulate together with the anion near the amide oxygen by forming solvent-shared ion pairs [15]. This effect is less pronounced for weakly hydrated cations (e.g., Na^+ and Cs^+), not just due to their weaker affinity for the amide oxygen, but also because cations do not readily come to nonpolar surfaces unless they arrive as a neutral ion pair with their counter anion [29, 32]. Indeed, Cs^+ and Na^+ do not readily partition to hydrophobic polymer surfaces, in part, because they pair relatively weakly with Cl^- compared to more strongly hydrated cations. Moreover, when paired with I^-, weakly hydrated cations like Cs^+ preferentially form ion pairs in the bulk solution. By contrast, Li^+ does not pair as well with I^-. As such, Li^+ is less depleted from the polymer interface, resulting in a weaker salting-out effect than is seen with CsI [31].

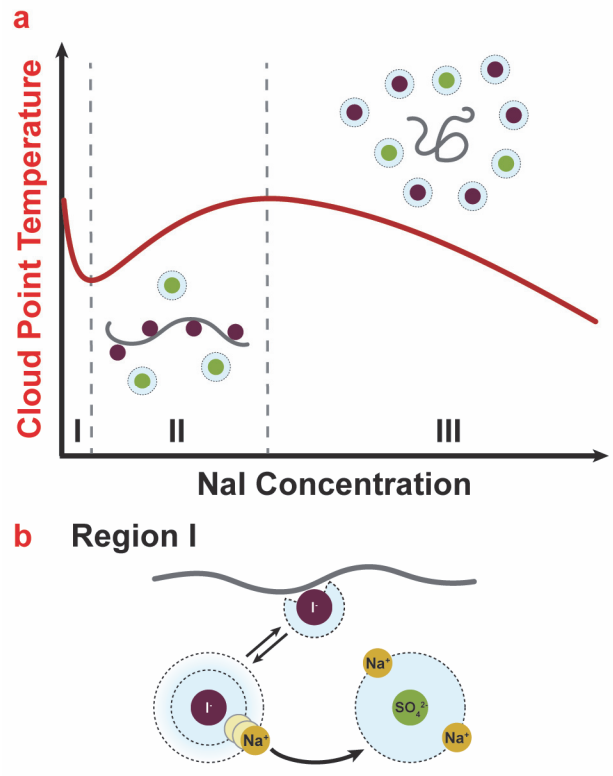

Fig. 1 a Schematic illustration of the cloud point temperature for PNIPAM (red curve) as a function of NaI concentration in a solution containing a fixed Na_2SO_4 concentration. The cloud point temperature curve can be divided into three concentration regimes, designated by the dashed gray vertical lines. The mechanism for the decrease in the cloud point temperature in region I is depicted schematically in **b**, whereby Na^+ preferentially partitions into the counterion cloud of SO_4^{2-}, leaving I^- more hydrated. In region II, the cloud point temperature increases as I^- is driven to the polymer/water interface. In region III, the cloud point temperature again decreases, because of a depleted volume effect. In both **a** and **b**, the light blue regions surrounded by black dashed circles represent ion hydration shells. The molecular level picture in **b** is not drawn to scale.

Polymer solubility in mixed salt solutions has been explored by others [33] as well as in our own laboratory [34]. The results indicate that substantial nonadditive behavior can arise. Specifically, the solubility of poly(*N*-isopropylacrylamide) (PNIPAM) was found to change in a complex fashion when NaI was introduced into a solution that already contained Na_2SO_4 [34]. PNIPAM is a thermoresponsive polymer which undergoes hydrophobic collapse above its cloud point temperature. The nonadditive mixed salt behavior originates from a competition for Na^+ between the two anions. Specifically, in the presence of Na_2SO_4, salting-out behavior is observed as NaI is added (Fig. 1a, region I). This is surprising because weakly hydrated anions like I^- are expected to shed their hydration water and interact directly with the hydrophobic polymer surface [4, 11, 12]. This favorable surface partitioning of I^- would salt PNIPAM into solution. Instead, the unexpected salting-out behavior can be attributed to the preferential partitioning of Na^+ to the counterion cloud around SO_4^{2-}, leaving I^- more hydrated (Fig. 1b). The more hydrated form of I^- preferentially partitions away from the polymer/water interface, thereby reducing the solubility of PNIPAM.

Upon further increasing the concentration of I^-, however, a salting-in effect occurs (Fig. 1a, region II). This happens because SO_4^{2-} becomes saturated with excess Na^+ and additional I^- is driven to the interface. Finally, at high NaI concentrations, the polymer/water interface becomes saturated with I^-. Therefore, further increases in NaI concentration lead to salting-out behavior via a depleted volume effect (Fig. 1a, region III). The molecular level mechanisms in all three regions have been verified using data taken by vibrational sum frequency spectroscopy as well as with all-atom molecular dynamics simulations [34].

In the presence of an anion from the middle of the Hofmeister series, such as Cl^-, the cationic Hofmeister series for the salting-out of PNIPAM would be $Na^+ > Cs^+ > K^+ > Li^+$ [15]. This result stands in contrast to the MI/M_2SO_4 systems explored herein with the same four cations, which is more complex. The cloud point temperature of PNIPAM is reported as a function of MI concentration in the presence and absence of 0.2 mol·L^{-1} M_2SO_4 for each cation. In all four mixed salt solutions, the cloud point curves follow the pattern shown in Fig. 1a. Because of the differences in cation pairing affinity with sulfate versus iodide, unusual cation specific behavior is observed. K^+ has the greatest relative affinity for SO_4^{2-} over I^-. As such, it gives rise to the most pronounced dip in region I, while Cs^+ leads to almost no dip at all. In region II, the cations compete with the polymer for pairing with I^-, resulting in the greatest salting-in behavior for K^+. Finally, salting-out behavior originating from an excluded volume effect is observed in region III and follows the more usual order: $Cs^+ > K^+ > Na^+ > Li^+$. This final ordering agrees with previous salting-out trends [31], because the binding sites for cations with SO_4^{2-} as well as I^- with PNIPAM are saturated at high MI concentrations.

2 Experimental

2.1 Chemicals Used

The chemicals used in this study are listed with their full name and accompanied by their chemical formula. The mass fraction purity is expressed as a percentage in parentheses. The purities of the chemicals are provided by the suppliers, and all chemicals were used without further purification. Lithium iodide (LiI, 99.9%), sodium iodide (NaI, 99.5%), cesium iodide (CsI, 99.9%) and sodium sulfate anhydrous (Na_2SO_4, ≥99%) were purchased from Sigma-Aldrich (St. Louis, MO). Potassium iodide (KI, ≥99%) was purchased from Acros Organics (Fair Lawn, NJ). Lithium sulfate anhydrous (Li_2SO_4, 99.7%), potassium sulfate (K_2SO_4, ≥99%) and cesium sulfate (Cs_2SO_4, 99%) were purchased from Alfa Aesar (Haverhill, MA). Poly(*N*-isopropylacrylamide) (PNIPAM) (M_v = 186 000 g·mol^{-1}; M_w/M_n = 2.63) was purchased from Polymer Source, Inc. (Quebec, Canada). Salts and polymer were dissolved in 18.2 MΩ·cm deionized water at the desired concentration. Deionized water was obtained from a NANOpure Ultrapure Water System (18.2 MΩ·cm, Barnstead, Dubuque, IA) and was purged with nitrogen gas to prevent the oxidation of iodide.

2.2 Sample Preparation

All samples were weighted on an analytical balance (Voyager VP214C, ± 0.0001 g, OHAUS Corporation, Newark, NJ). 50 mL of the stock solution of 10 mg·mL^{-1} PNIPAM was prepared and aliquoted into 100 μL samples, which were stored in microcentrifuge tubes. The polymer samples were concentrated into pellets using a refrigerated vacuum concentrator (Savant SPD111V-P1 SpeedVac Kit, Thermo Fisher Scientific, Waltham, MA). Appropriate volumes of salt stock solutions and deionized water were introduced to the polymer pellets to reach a final volume of 100 μL at the desired salt concentration. The samples were vortexed to ensure homogenous mixing and then stored overnight at 4 ºC before measurements were made. Samples for this study could be divided into three categories: (1) PNIPAM in water, (2) PNIPAM in single salt solutions (iodide or sulfate salt), and (3) PNIPAM in mixed iodide/sulfate solutions. The cations employed in this study include Li^+, Na^+, K^+, and Cs^+.

2.3 Cloud Point Temperature Measurements

Changes in the turbidity of solutions containing 10 mg·mL^{-1} PNIPAM at the desired salt concentration were measured as a function of temperature using an automated melting point apparatus (OptiMelt MPA 100, Stanford Research Systems) at ambient pressure. In a typical experiment, three capillary tubes, each containing 10 μL of the sample, were place side-by-side into the apparatus. The capillary tubes were purchased from Kimble Chase LLC (Vineland, NJ) and had dimensions of 1.5−1.8 mm × 90 mm. A temperature ramp rate of 1 ºC·min^{-1} was employed in all cases. Built-in data processing software recorded light scattering curves as a function of temperature. The scattering intensity was low at temperatures below the cloud point temperature of the sample. The intensity increased sharply near the cloud point temperature and eventually reached a constant value as the temperature was further increased. The cloud point temperature was taken to be the onset of the light scattering intensity increase relative to the baseline that was observed at colder temperatures. The cloud point temperature was measured for each solution condition at least three times, and the mean value was taken. The measurements had a typical standard error of ± 0.1 ºC.

3 Results and Discussion

Figure 2 displays cloud point temperature (T_c) values for PNIPAM in the presence of single and mixed salt solutions with four cations: Li^+, Na^+, K^+ and Cs^+. The raw data can be found in Tables S1-S3 in the Supporting Information. Anion specific effects on the cloud point of PNIPAM can readily be seen by comparing the shape of the curves for iodide and for sulfate in Figs. 2a and 2b, respectively. As MI salt is added to the solution, the cloud point of PNIPAM initially increases, reaches a maximum and then decreases for all four iodide salts (Fig. 2a), consistent with previous data [31]. The shape of the cloud point curves

can be explained by the partitioning of I^- to the polymer/water interface. Upon saturation, the introduction of additional MI leads to salting-out behavior via a depleted volume effect. By contrast, the cloud point temperature of PNIPAM decreases in a nearly linear fashion for all four cations as the M_2SO_4 concentration is increased (Fig. 2b). This occurs because SO_4^{2-} is strongly depleted from the polymer/water interface with all four salts.

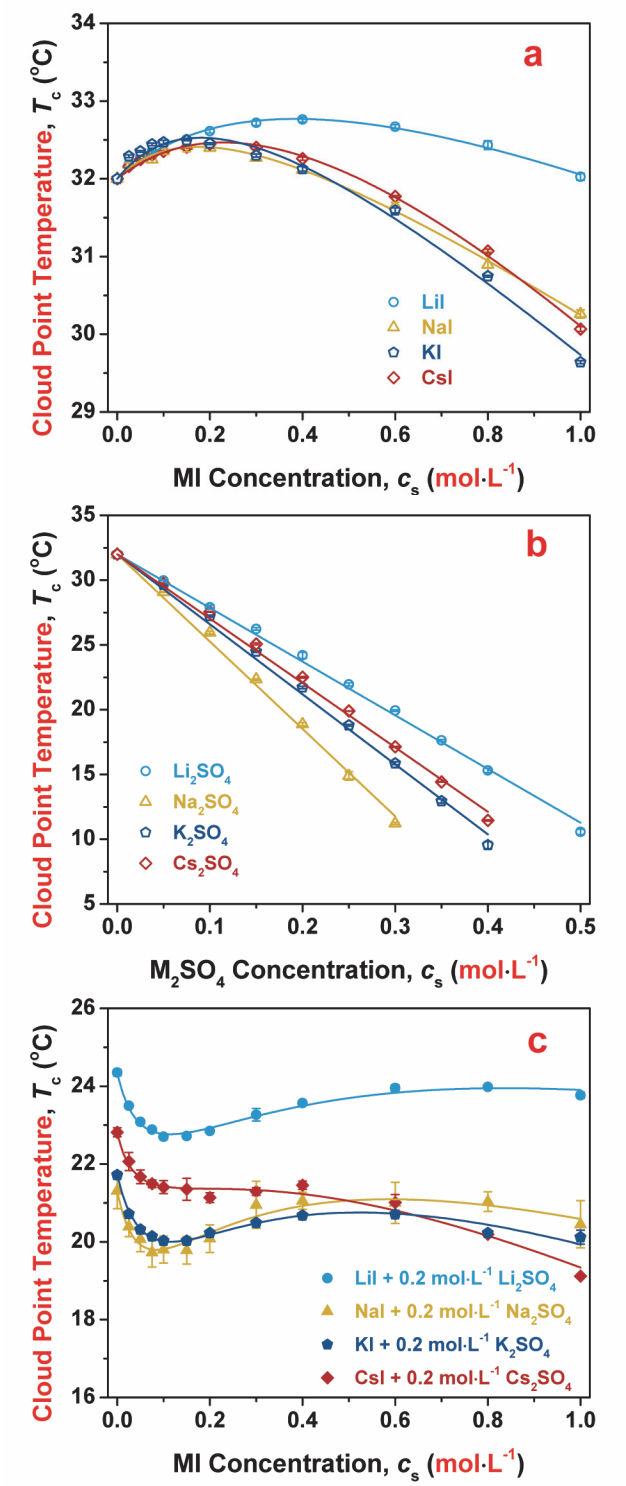

Significantly, titrating MI into PNIPAM solutions that already contain 0.2 mol·L^{-1} M_2SO_4 leads to cloud point temperature behavior that is dramatically different from the curves with either MI alone or M_2SO_4 alone (Fig. 2c). In other words, the observed behavior in Fig. 2c does not represent the simple additive sum of the effects of the individual salts. Such nonadditivity is most clearly manifest as a dip in the cloud point temperature at low MI concentrations. Upon further increase in the MI concentration, the cloud point temperature increases, reaches a maximum and eventually decreases. As can be seen, the cation identity strongly influences the shape of the individual cloud point temperature curves by governing the magnitude of the dip, the subsequent rise, as well as the salting-out slopes at higher concentrations

Fig. 2 Cloud point temperature (T_c) for 10 mg·mL^{-1} PNIPAM solutions as a function of **a** MI concentration, **b** M_2SO_4 concentration, and **c** MI concentration in the presence of 0.2 mol·L^{-1} M_2SO_4. M^+ represents the four alkali metal cations, namely Li^+, Na^+, K^+ and Cs^+. The error bars correspond to standard deviations from three measurements. These error bars are smaller than the symbols in cases where they are not visible. In **a** and **c**, the solid lines are fits of the data to Eq. 1, and the fitting parameters are reported in Table 1. The solid lines in **b** are fits to the data with straight lines, and the slopes are (-41.5 ± 0.3) °C·mol^{-1}·L, (-67.4 ± 0.4) °C·mol^{-1}·L, (-54.1 ± 0.2) °C·mol^{-1}·L and (-49.7 ± 0.1) °C·mol^{-1}·L for Li^+, Na^+, K^+ and Cs^+, respectively. The errors associated with these slopes are the standard deviations from three individual fits of three experimental trials.

In order to quantitatively compare the effects of the four cations, the cloud point temperature (T_c) can be modeled as a function of MI concentration (c_s):

$$T_c = T_0 + ac_s + \frac{B_{max,1}c_s}{K_{D,1} + c_s} + \frac{B_{max,2}c_s}{K_{D,2} + c_s} \quad (1)$$

where T_0 is the cloud point temperature in the absence of MI, while a is a constant which correlates to the linear surface tension increment at the polymer/water interface. The third term, which resembles a Langmuir binding isotherm, accounts for the increase in the cloud point due to iodide adsorption to the polymer surface. This term reaches its maximum value, $B_{max,1}$, when all the binding sites on the polymer chains are saturated. The dissociation constant, $K_{D,1}$, quantifies the strength of I^- binding to the polymer. The first three terms are sufficient to model the data in Fig. 2a. The fourth term is required to capture the nonadditivity at low iodide concentrations in mixed salt solutions (Fig. 2c). This term is also reminiscent of a Langmuir binding isotherm but originates from enhanced iodide hydration in the bulk [34]. The values obtained for $B_{max,2}$ are negative, which reflect the decrease in the cloud point temperature of PNIPAM at low iodide concentrations. The dissociation constant $K_{D,2}$ arises from the competition for the cations between iodide and sulfate, which in turn leaves I^- more hydrated. In fact, as I^- becomes more hydrated, it is repelled from the polymer/water interface and leads to a salting-out effect. The equilibrium dissociation constants $K_{D,1}$ and $K_{D,2}$ discussed herein represent apparent affinities for ion-polymer and ion-ion interactions, respectively. These interactions represent averages over various sites and could involve contact pairing as well as solvent shared pair formation. Equation 1 was previously employed to model the cloud point data for iodide/sulfate mixtures with Na^+ being the common cation [34]. The cloud point temperature shown in Figs. 2a and 2c was fit to Eq. 1 and the fitting parameters are summarized in Table 1.

Table 1 Fitting parameters (T_0, a, $B_{max,1}$, $K_{D,1}$, $B_{max,2}$, $K_{D,2}$) from Eq. 1 for the cloud point temperature (T_c) of PNIPAM as a function of the concentration (c_s) for four metal iodide salts, LiI, NaI, KI and CsI, in the absence and presence of 0.2 mol·L^{-1} Li_2SO_4, Na_2SO_4, K_2SO_4 and Cs_2SO_4, respectively[a].

	Single Salt				**Mixed Salts**			
Fitting Parameter	**LiI**	**NaI**	**KI**	**CsI**	**LiI + 0.2 mol·L^{-1} Li_2SO_4**	**NaI + 0.2 mol·L^{-1} Na_2SO_4**	**KI + 0.2 mol·L^{-1} K_2SO_4**	**CsI + 0.2 mol·L^{-1} Cs_2SO_4**
T_0 (°C)	32.0 ± 0.0	32.0 ± 0.0	32.0 ± 0.0	32.0 ± 0.0	24.4 ± 0.1	21.3 ± 0.5	21.7 ± 0.1	22.8 ± 0.1
a (°C·mol^{-1}·L)	-3.0 ± 0.3	-4.2 ± 0.2	-5.6 ± 0.4	-7.1 ± 0.4	-3.0 ± 0.3	-4.2 ± 0.2	-5.6 ± 0.4	-7.1 ± 0.4
$B_{max,1}$ (°C)	4.8 ± 0.6	3.2 ± 0.3	4.4 ± 0.6	9.5 ± 1.2	12.0 ± 0.4	16.1 ± 2.3	20.6 ± 1.4	11.6 ± 0.6
$K_{D,1}$ (mol·L^{-1})	0.57 ± 0.07	0.31 ± 0.04	0.34 ± 0.06	0.80 ± 0.09	0.57 ± 0.07	0.31 ± 0.04	0.34 ± 0.06	0.80 ± 0.09
$B_{max,2}$ (°C)	-	-	-	-	-5.5 ± 0.3	-9.7 ± 2.1	-13.0 ± 1.3	-2.9 ± 0.3
$K_{D,2}$ (mol·L^{-1})	-	-	-	-	0.08 ± 0.01	0.09 ± 0.02	0.12 ± 0.01	0.05 ± 0.01

[a]Three trials of the cloud point temperature data were fitted individually, and the reported fitted values are the average of three trials. The uncertainties reported herein correspond to the propagated errors from the three fitted trials. The uncertainty associated with T_0 in the absence of salt is 0.0 because the three measurements yielded the same values.

3.1 Salting-out order of alkali metal sulfate salts

As can be seen in Fig. 2b, the salting-out order for sulfate salts is $Na^+ > K^+ > Cs^+ > Li^+$, consistent with the order of the first data points on the curves in Fig. 2c. This result differs from the consensus direct cationic Hofmeister series $Cs^+ > K^+ > Na^+ > Li^+$ [16], which more typically occurs at a charged surface. In the present case, Cs^+ and Na^+ have switched places. Moreover, reordering of the cationic Hofmeister series at uncharged polymer surfaces has been observed previously with chloride [15] and iodide counterions [31]. The cation-specific effects in these two cases were attributed to the propensity of the individual cations to form ion pairs at the polymer surface with Cl^- and in the bulk solution with I^-. By analogy, reordering of the series with sulfate as the counterion should arise from the balance between cation-sulfate ion-pairing in the bulk and cation-polymer interactions. Table 2 lists the literature values for the 1:1 dissociation constants (K_d) of the four cation-sulfate pairs in water [35–37]. As can be seen, Li^+, Na^+, and K^+, all have similar interactions with SO_4^{2-}, but Cs^+ interacts three times more weakly. Moreover, SO_4^{2-} is strongly excluded from the polymer/water interface. As such, SO_4^{2-} does not help partition Cs^+ away from the interface nearly as effectively as it can for the other three cations. Nevertheless, Cs_2SO_4 is not the least effective salt for salting out PNIPAM. That designation goes to Li_2SO_4. Indeed, Li^+, which is more strongly hydrated, can form weak but favorable interactions with the amide oxygen on the polymer, while Cs^+ hardly interacts with the amide at all [13, 15]. As such, the salting-out order of the four cation sulfate salts stems from a competition for the cations between the amide oxygen and the strongly excluded sulfate counterions.

Table 2 Literature values for the 1:1 dissociation constant (K_d) of the four cations (Li^+, Na^+, K^+, Cs^+) with sulfate (SO_4^{2-}) and with iodide (I^-). The values are calculated from activity coefficient data obtained from electrical conductivity measurements at 25 °C and ambient pressure.

Cation Identity	**Dissociation Constant K_d (mol·L^{-1})**	
	SO_4^{2-}	**I^-**
Li^+	0.17[a]	1.85[b]
Na^+	0.15[a]	2.94[c]
K^+	0.14[a]	1.41[c]
Cs^+	0.47[a]	0.75[c]

[a]Values were obtained from ref [35]. [b]Value was obtained from ref [36]. [c]Values were obtained from ref [37].

3.2 Region I: Sulfate and iodide compete for the cation

For the mixed salt case (Fig. 2c), the magnitude of the dip in region I is reflected in the $B_{max,2}$ value and follows the salting-out order $K^+ > Na^+ > Li^+ > Cs^+$ (see Table 1). As noted above, the salting-out trend found in this region originates from enhanced I^- hydration in the bulk solution, related to the swiping of cations from I^- by SO_4^{2-} [34]. As such, a competitive binding model [38] can be employed to qualitatively compare the relative fraction of more hydrated iodide ions in the four salt mixtures. Figure 3a schematically illustrates the competition for the cations (gray) between sulfate (green) and iodide (purple). Assuming 1:1 binding stoichiometry of the cation with sulfate as well as with iodide, the binding equilibria are given by:

$$M^+ + SO_4^{2-} \overset{K_1}{\rightleftharpoons} MSO_4^-$$

$$M^+ + I^- \overset{K_2}{\rightleftharpoons} MI$$

where K_1 and K_2 represent the equilibrium association constants of the cation with sulfate and with iodide, respectively. If the concentration of sulfate is $[SO_4^{2-}]$ and the concentration of iodide is $[I^-]$, then the corresponding binding polynomial, Q, can be expressed as:

$$Q = 1 + K_1[SO_4^{2-}] + K_2[I^-] \tag{2}$$

where Q is a binding partition function, summing over all possible states of the cations. Q has a value of 1 when none of the cations are bound to anions. The number of configurations rises as sulfate and iodide become associated with the cations, represented by the next two terms, respectively. The concentration of more hydrated iodide ions depends on the ability of sulfate to swipe cations from iodide, which is proportional to the fraction of cations bound to sulfate:

$$f_{MSO_4^-} = \frac{K_1[SO_4^{2-}]}{Q} = \frac{K_1[SO_4^{2-}]}{1 + K_1[SO_4^{2-}] + K_2[I^-]} \tag{3}$$

The fraction of states with sulfate-bound cations ($f_{MSO_4^-}$) can be computed using Eq. 3 and the known dissociation constants, K_d, for the cation-sulfate and cation-iodide pairs (Table 2). Since K_1 and K_2 represent association constants, they are equal to the inverse of the dissociation constant values reported in Table 2. The concentration of sulfate is fixed at 0.2 mol·L^{-1} in this analysis, while the concentration of iodide varies between 0.0 mol·L^{-1} and 0.3 mol·L^{-1}, corresponding to the concentration range at which nonadditivity is most strongly observed in Fig. 2c. Indeed, SO_4^{2-} becomes saturated with M^+ at higher MI concentrations.

The fraction of cations bound to SO_4^{2-} is plotted in Fig. 3b and follows the order $K^+ > Na^+ > Li^+ > Cs^+$, although Na^+ begins to overtake K^+ near the end of this range. The fraction of cations bound to SO_4^{2-} agrees with the salting-out ordering found for the $B_{max,2}$ values in the four salt mixtures (Table 1). Significantly, the fraction of Cs^+ bound to SO_4^{2-} is considerably lower than the values for the other three cations. In fact, the value for Cs^+ is only just over half of its value for the other three cations. This correlates well with the lack of a dip seen in the CsI/Cs_2SO_4 data in Fig. 2c. This difference between Cs^+ and the other three cations, however, does not quantitatively correlate to the $B_{max,2}$ values (Table 1). Instead, the magnitude of the dip changes more evenly across the four cations. The discrepancy between the binding partition function analysis and the cloud point data points to the limitations of this competitive binding model to describe the behavior of ions in mixed salt solutions. Specifically, it only accounts for the first cation-sulfate binding event, and therefore underestimates the fraction of cations bound to sulfate in the presence of iodide. Once the first cation binds to sulfate, the subsequent cation-sulfate dissociation constants are undoubtedly weaker. It is, however, difficult to obtain these values. Nevertheless, the

competitive binding model presumably would provide greater quantitative accuracy if these values were known.

Next, the dissociation constant $K_{D,2}$ arises from the competition for the cations between iodide and sulfate, which in turn leaves I^- more hydrated. Nevertheless, the measured $K_{D,2}$ values are identical within experimental error for the four cation systems (Table 1). It has been shown previously with the Na^+ system that the measured $K_{D,2}$ value is tightly correlated to the background concentration of Na_2SO_4 [34]. Specifically, the measured $K_{D,2}$ value is found to be approximately half the concentration of the strongly hydrated anions introduced at the start of the experiment. The identity of the common cation employed in these measurements should modulate this value, but the results in Fig. 2c and Table 1 indicate that cloud point measurements are not sensitive enough to distinguish such differences. Instead, $B_{max,2}$ is the more sensitive metric of cation specific effects.

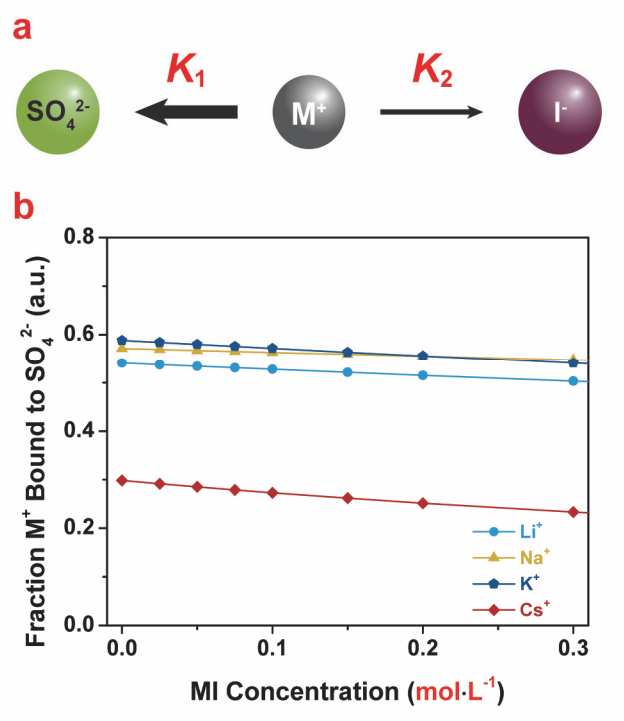

Fig. 3 a Schematic illustration of the competition for cations between SO_4^{2-} and I^-. **b** The fraction of cations bound to SO_4^{2-} computed using Eq. 3 and the dissociation constants reported in Table 2.

3.3 Region II: Iodide preferentially adsorbs to the polymer surface

After SO_4^{2-} becomes saturated with cations, the salting-in effect caused by iodide's preferential partitioning to the polymer/water interface becomes the dominant contribution to changes in the cloud point data. As can be seen in Table 1, the $K_{D,1}$ values show that I^- binds tightest to the polymer when paired with Na^+ and K^+. Li^+ gives rise to intermediate behavior, while I^- binds weakest when Cs^+ is the counterion. This is essentially the opposite order to the one seen for metal cation interactions with I^- (Table 2), for which Cs^+ binds most tightly and Na^+ shows the weakest interaction. These results are consistent with the notion that iodide-polymer interactions are modulated by I^- interactions with the metal counterions out in the bulk solution [31].

Next, the saturable increase in the cloud point upon I^- binding to the polymer surface is quantified by the $B_{max,1}$ value (Table 1). The presence of strongly hydrated SO_4^{2-} ions helps force I^- out of the bulk solution and toward the polymer/water interface [34, 39]. The $B_{max,1}$ values, which correspond to the extent of loading of I^- on the polymer surface, are larger in each case for the four salt mixtures compared to the simple MI cases (Table 1). In other words, enhanced I^- adsorption leads to a more pronounced increase in

the cloud point temperature when sulfate is present. Curiously, even though the presence of M_2SO_4 causes a substantial increase in the $B_{max,1}$ values, it does not give rise to a detectable change in the $K_{D,1}$ values for the mixed salt cases versus those with just MI (Table 1). This is analogous to the results in region I where $B_{max,2}$ was also more sensitive to specific cation effects than $K_{D,2}$. In the current case, these results mean that cloud point measurements are more sensitive to slight changes in I^- loading as opposed to changes in the corresponding equilibrium dissociation constants. Previously, changes in both the iodide loading as well as the iodide-polymer dissociation constant value in the presence of Na_2SO_4 were detected by using vibrational sum frequency spectroscopy measurements [34]. This would indicate that interfacial water structure is more sensitive to differences in ion affinities compared to macroscopic phase transition measurements.

3.4 Region III: Excluded volume effect salts PNIPAM out of solution

The salting-out of PNIPAM at high salt concentrations has been shown to correlate with the surface tension increment of individual salts and is captured by the *a* coefficients, which have negative values (Table 1) [4]. The cation-dependent salting-out trend for I^- originates from a competition for this anion between cations in the bulk solution and the hydrophobic moieties on the polymer surface [31]. The trend is in partial agreement with the cation-iodide pairing affinity series $Cs^+ > K^+ > Li^+ > Na^+$ (Table 2). However, despite having stronger affinity for I^- compared to Na^+, Li^+ switches place in the series to become the least effective salting-out species, giving rise to the salting-out order: $Cs^+ > K^+ > Na^+ > Li^+$. This final rank ordering occurs because Li^+ can form weak but favorable interaction with the amide oxygen on the polymer, which helps mitigate the partitioning of I^- away from the polymer/water interface and thereby attenuates the salting out effect [15, 31].

4 Conclusion

Using PNIPAM as a model system, we have demonstrated that the identity of the cation plays a key role in the nonadditive behavior of salt mixtures containing I^- and SO_4^{2-}. Specifically, in region I, the difference in the ion pairing affinity of the cation with SO_4^{2-} versus I^- determines the extent to which the cation is partitioned out of the counterion cloud around I^-, which, in turn determines the concentration of more hydrated I^-. The cation pairing affinity to SO_4^{2-} follows the order $K^+ \approx Na^+ \approx Li^+ > Cs^+$, which is markedly different from the cation pairing with iodide: $Cs^+ > K^+ > Li^+ > Na^+$. Using a competitive binding model, we have shown that the concentration of I^- with enhanced hydration follows the series $K^+ > Na^+ > Li^+ > Cs^+$. This ordering explains the relatively strong salting-out behavior seen with K^+ counterions in region I. Upon increasing the MI concentration, SO_4^{2-} becomes saturated with metal counterions and salts

I^- out of solution and toward the polymer/water interface (region II). This enhanced driving force is manifest by the larger $B_{max,1}$ values in salt mixtures compared to those in single salt solutions. In region III, after the polymer surface becomes saturated with I^-, the excluded volume effect drives the salting-out behavior in all four salt mixtures. In this final concentration regime, Cs^+ operates as the strongest salting-out agent, because it pairs most effectively with I^-. The results reported herein suggest that the behavior of complex electrolyte solutions arises from a complex balance amongst ion-ion, ion-polymer, and ion-water interactions.

Acknowledgements

The authors would like to thank Dr. Bradley Rogers for the helpful discussions. This work was funded by the National Science Foundation (CHE-2004050).

References

1. Hofmeister, F.: Zur Lehre von der Wirkung der Salze. Arch. Für Exp. Pathol. Pharmakol. 24, 247–260 (1888). https://doi.org/10.1007/BF01918191
2. Kunz, W., Henle, J., Ninham, B.W.: 'Zur Lehre von der Wirkung der Salze' (About the Science of the Effect of Salts): Franz Hofmeister's Historical Papers. Curr. Opin. Colloid Interface Sci. 9, 19–37 (2004). https://doi.org/10.1016/j.cocis.2004.05.005
3. Zhang, Y., Cremer, P.S.: Chemistry of Hofmeister Anions and Osmolytes. Annu. Rev. Phys. Chem. 61, 63–83 (2010). https://doi.org/10.1146/annurev.physchem.59.032607.093635
4. Zhang, Y., Furyk, S., Bergbreiter, D.E., Cremer, P.S.: Specific Ion Effects on the Water Solubility of Macromolecules: PNIPAM and the Hofmeister Series. J. Am. Chem. Soc. 127, 14505–14510 (2005). https://doi.org/10.1021/ja0546424
5. Jungwirth, P., Winter, B.: Ions at Aqueous Interfaces: From Water Surface to Hydrated Proteins. Annu. Rev. Phys. Chem. 59, 343–366 (2008). https://doi.org/10.1146/annurev.physchem.59.032607.093749
6. Heyda, J., Vincent, J.C., Tobias, D.J., Dzubiella, J., Jungwirth, P.: Ion Specificity at the Peptide Bond: Molecular Dynamics Simulations of N-Methylacetamide in Aqueous Salt Solutions. J. Phys. Chem. B. 114, 1213–1220 (2010). https://doi.org/10.1021/jp910953w
7. Rembert, K.B., Paterová, J., Heyda, J., Hilty, C., Jungwirth, P., Cremer, P.S.: Molecular Mechanisms of Ion-Specific Effects on Proteins. J. Am. Chem. Soc. 134, 10039–10046 (2012). https://doi.org/10.1021/ja301297g
8. Okur, H.I., Hladílková, J., Rembert, K.B., Cho, Y., Heyda, J., Dzubiella, J., Cremer, P.S., Jungwirth, P.: Beyond the Hofmeister Series: Ion-Specific Effects on Proteins and Their Biological Functions. J. Phys. Chem. B. 121, 1997–2014 (2017). https://doi.org/10.1021/acs.jpcb.6b10797
9. Jungwirth, P., Tobias, D.J.: Specific Ion Effects at the Air/Water Interface. Chem. Rev. 106, 1259–1281 (2006). https://doi.org/10.1021/cr0403741
10. Pegram, L.M., Record, M.T.: Thermodynamic Origin of Hofmeister Ion Effects. J. Phys. Chem. B. 112, 9428–9436 (2008). https://doi.org/10.1021/jp800816a
11. Cho, Y., Zhang, Y., Christensen, T., Sagle, L.B., Chilkoti, A., Cremer, P.S.: Effects of Hofmeister Anions on the Phase Transition Temperature of Elastin-like Polypeptides. J. Phys. Chem. B. 112, 13765–13771 (2008). https://doi.org/10.1021/jp8062977
12. Rembert, K.B., Okur, H.I., Hilty, C., Cremer, P.S.: An NH Moiety Is Not Required for Anion Binding to Amides in Aqueous Solution. Langmuir. 31, 3459–3464 (2015). https://doi.org/10.1021/acs.langmuir.5b00127

13. Okur, H.I., Kherb, J., Cremer, P.S.: Cations Bind Only Weakly to Amides in Aqueous Solutions. J. Am. Chem. Soc. 135, 5062–5067 (2013). https://doi.org/10.1021/ja3119256
14. Pluhařová, E., Baer, M.D., Mundy, C.J., Schmidt, B., Jungwirth, P.: Aqueous Cation-Amide Binding: Free Energies and IR Spectral Signatures by Ab Initio Molecular Dynamics. J. Phys. Chem. Lett. 5, 2235–2240 (2014). https://doi.org/10.1021/jz500976m
15. Bruce, E.E., Okur, H.I., Stegmaier, S., Drexler, C.I., Rogers, B.A., van der Vegt, N.F.A., Roke, S., Cremer, P.S.: Molecular Mechanism for the Interactions of Hofmeister Cations with Macromolecules in Aqueous Solution. J. Am. Chem. Soc. 142, 19094–19100 (2020). https://doi.org/10.1021/jacs.0c07214
16. Traube, J.: The Attraction Pressure. J. Phys. Chem. 14, 452–470 (1910). https://doi.org/10.1021/j150113a003
17. Vrbka, L., Vondrášek, J., Jagoda-Cwiklik, B., Vácha, R., Jungwirth, P.: Quantification and Rationalization of the Higher Affinity of Sodium over Potassium to Protein Surfaces. Proc. Natl. Acad. Sci. 103, 15440–15444 (2006). https://doi.org/10.1073/pnas.0606959103
18. Hess, B., Vegt, N.F.A. van der: Cation Specific Binding with Protein Surface Charges. Proc. Natl. Acad. Sci. 106, 13296–13300 (2009). https://doi.org/10.1073/pnas.0902904106
19. Kherb, J., Flores, S.C., Cremer, P.S.: Role of Carboxylate Side Chains in the Cation Hofmeister Series. J. Phys. Chem. B. 116, 7389–7397 (2012). https://doi.org/10.1021/jp212243c
20. Zhang, Y., Furyk, S., Sagle, L.B., Cho, Y., Bergbreiter, D.E., Cremer, P.S.: Effects of Hofmeister Anions on the LCST of PNIPAM as a Function of Molecular Weight. J. Phys. Chem. C. 111, 8916–8924 (2007). https://doi.org/10.1021/jp0690603
21. Zhang, Y., Cremer, P.S.: The Inverse and Direct Hofmeister Series for Lysozyme. Proc. Natl. Acad. Sci. 106, 15249–15253 (2009). https://doi.org/10.1073/pnas.0907616106
22. Janc, T., Lukšič, M., Vlachy, V., Rigaud, B., Rollet, A.-L., Korb, J.-P., Mériguet, G., Malikova, N.: Ion-Specificity and Surface Water Dynamics in Protein Solutions. Phys. Chem. Chem. Phys. 20, 30340–30350 (2018). https://doi.org/10.1039/C8CP06061D
23. Janc, T., Korb, J.-P., Lukšič, M., Vlachy, V., Bryant, R.G., Mériguet, G., Malikova, N., Rollet, A.-L.: Multiscale Water Dynamics on Protein Surfaces: Protein-Specific Response to Surface Ions. J. Phys. Chem. B. 125, 8673–8681 (2021). https://doi.org/10.1021/acs.jpcb.1c02513
24. Rogers, B.A., Okur, H.I., Yan, C., Yang, T., Heyda, J., Cremer, P.S.: Weakly Hydrated Anions Bind to Polymers but not Monomers in Aqueous Solutions. Nat. Chem. In press (2021). https://doi.org/10.1038/s41557-021-00805-z
25. Guggenheim, E.A.: The Specific Thermodynamic Properties of Aqueous Solutions of Strong Electrolytes. Lond. Edinb. Dublin Philos. Mag. J. Sci. 19, 588–643 (1935). https://doi.org/10.1080/14786443508561403
26. Guggenheim, E.A., Turgeon, J.C.: Specific Interaction of Ions. Trans. Faraday Soc. 51, 747–761 (1955). https://doi.org/10.1039/TF9555100747
27. Brönsted, J.N.: Studies on Solubility. IV. The Principle of the Specific Interation of Ions. J. Am. Chem. Soc. 44, 877–898 (1922). https://doi.org/10.1021/ja01426a001
28. Brönsted, J.N.: The Individual Thermodynamic Properties of Ions. J. Am. Chem. Soc. 45, 2898–2910 (1923). https://doi.org/10.1021/ja01665a015
29. Collins, K.D., Washabaugh, M.W.: The Hofmeister Effect and the Behaviour of Water at Interfaces. Q. Rev. Biophys. 18, 323–422 (1985). https://doi.org/10.1017/S0033583500005369
30. Heyda, J., Okur, H.I., Hladílková, J., Rembert, K.B., Hunn, W., Yang, T., Dzubiella, J., Jungwirth, P., Cremer, P.S.: Guanidinium can both Cause and Prevent the Hydrophobic Collapse of Biomacromolecules. J. Am. Chem. Soc. 139, 863–870 (2017). https://doi.org/10.1021/jacs.6b11082
31. Bruce, E.E., Bui, P.T., Cao, M., Cremer, P.S., van der Vegt, N.F.A.: Contact Ion Pairs in the Bulk Affect Anion Interactions with Poly(N-isopropylacrylamide). J. Phys. Chem. B. 125, 680–688 (2021). https://doi.org/10.1021/acs.jpcb.0c11076
32. Collins, K.D.: Charge Density-Dependent Strength of Hydration and Biological Structure. Biophys. J. 72, 65–76 (1997). https://doi.org/10.1016/S0006-3495(97)78647-8

33. Moghaddam, S.Z., Thormann, E.: Hofmeister Effect of Salt Mixtures on Thermo-Responsive Poly(propylene oxide). Phys. Chem. Chem. Phys. 17, 6359–6366 (2015). https://doi.org/10.1039/C4CP05677A
34. Bruce, E.E., Bui, P.T., Rogers, B.A., Cremer, P.S., van der Vegt, N.F.A.: Nonadditive Ion Effects Drive Both Collapse and Swelling of Thermoresponsive Polymers in Water. J. Am. Chem. Soc. 141, 6609–6616 (2019). https://doi.org/10.1021/jacs.9b00295
35. Reardon, E.J.: Dissociation Constants of Some Monovalent Sulfate Ion Pairs at 25 Deg From Stoichiometric Activity Coefficients. J. Phys. Chem. 79, 422–425 (1975). https://doi.org/10.1021/j100572a005
36. Fuoss, R.M.: Conductimetric Determination of Thermodynamic Pairing Constants for Symmetrical Electrolytes. Proc. Natl. Acad. Sci. 77, 34–38 (1980). https://doi.org/10.1073/pnas.77.1.34
37. Gujt, J., Bešter-Rogač, M., Hribar-Lee, B.: An Investigation of Ion-Pairing of Alkali Metal Halides in Aqueous Solutions Using the Electrical Conductivity and the Monte Carlo Computer Simulation Methods. J. Mol. Liq. 190, 34–41 (2014). https://doi.org/10.1016/j.molliq.2013.09.025
38. Felitsky, D.J., Record, M.T.: Application of the Local-Bulk Partitioning and Competitive Binding Models to Interpret Preferential Interactions of Glycine Betaine and Urea with Protein Surface. Biochemistry. 43, 9276–9288 (2004). https://doi.org/10.1021/bi049862t
39. Ottosson, N., Heyda, J., Wernersson, E., Pokapanich, W., Svensson, S., Winter, B., Öhrwall, G., Jungwirth, P., Björneholm, O.: The Influence of Concentration on the Molecular Surface Structure of Simple and Mixed Aqueous Electrolytes. Phys. Chem. Chem. Phys. 12, 10693–10700 (2010). https://doi.org/10.1039/C0CP00365D

Table of Contents Graphic